JOURNAL OF SOLID STATE CHEMISTRY 36, 139–147 (1981)

The Structure of $LaTaO_4$ at 300°C by Neutron Powder Profile Analysis

R. J. CAVA[1] AND R. S. ROTH

National Bureau of Standards, Washington, D.C. 20234

Received February 4, 1980; in final form May 6, 1980.

$LaTaO_4$ above 175°C is orthorhombic, space group $A2_1am$, with $a = 5.6643(1)$, $b = 14.6411(3)$, $c = 3.9457(1)$, and $Z = 4$. It is isostructural with room temperature $BaMnF_4$. The structure, refined by the Rietveld powder profile analysis technique to a final agreement index of 8.6%, consists of sheets of corner shared TaO_6 octahedra extending perpendicular to b, bonded to each other parallel to b by the nine coordinated lanthanum ions. All atoms are in position $(x, y, 0)$ with coordinates: La (0.1788, 0.1676), Ta (0.2192, 0.4141, O1 (0.4216, 0.3008), O2 (−0.0486, 0.3380), O3 (0.5614, 0.4689), O4 (0.2496, 0.9153). Orthorhombic $CeTaO_4$ and $PrTaO_4$ are isostructual.

Introduction

Compounds of stoichiometry ABO_4, where A are rare earth ions and B is niobium or tantalum, occur in two structure types. The niobates and all but the La, Ce, and Pr tantalates display a monoclinic distortion of the scheelite structure at room temperature (*1, 2*). The La, Ce, and Pr tantalates have the monoclinic $LaTaO_4$ structure type at room temperature (*3*). We suspected the presence of a phase transformation in these materials due to our observation of an orthorhombic phase of $LaTaO_4$ on growing crystals from a molybdenum oxide flux, and the twinning of $CeTaO_4$ crystals on cooling from the melt (*2*). A monoclinic–orthorhombic phase change was subsequently found and characterized by high-temperature powder X-ray diffraction for all three compounds (*4*).

These compounds are of particular interest because the cerium members $CeTaO_4$ and $CeNbO_4$ undergo rapid oxidation at moderate temperatures (*5*) and form phases in which mixed Ce^{3+} and Ce^{4+} valence states occur. For this reason it has been proposed that these structure types might exhibit high oxygen ion and electronic conductivity. We have been able to accommodate significant quantities of excess oxygen in both $LaTaO_4$ and $LaNbO_4$ by the substitution of Th^{4+} for La^{3+} and W^{6+} for Nb^{5+} and Ta^{5+}. This accommodation causes the occurrence of a modulated structure in the niobate (*6*) and is apparently via a solid solution in the tantalate. Measurement of the conductivities of these materials is presently underway and will be reported in subsequent papers, but tentative results for the niobates do not indicate a conductivity characteristic of fast ion oxygen transport.

The monoclinic to orthorhombic phase transformations in the La, Ce, and Pr tantalates display significant hysteresis. The transition temperatures on heating and

[1] Present address: Bell Laboratories, 600 Mountain Avenue, Murray Hill, New Jersey 07974.

0022-4596/81/020139-09$02.00/0

cooling are 175/150°C for $LaTaO_4$, 818/729°C for $CeTaO_4$, and 1300/1205°C for $PrTaO_4$. We chose $LaTaO_4$ as the model for the orthorhombic structure type due to our success in doping it with excess oxygen, and its easily accessible transition temperature.

Experimental

Several attempts were made at pulling $LaTaO_4$ from the melt (m.p. 2100°C). Although boules of considerable size could be drawn, they invariably shattered on cooling to room temperature, independently of cooling rate between several minutes and several hours. We believe that the shattering occurs at the phase transition, although we did not monitor the process in any detail.

Small fragments could be recovered from the shattered boules, and several of these were studied on a precession camera equipped with a furnace capable of attaining temperatures of up to about 500°C. The single crystal photographs at 200°C exhibited the extinctions: $hkl: h + k \neq 2n$ and $h0l: l \neq 2n$, consistent with the space groups $Cmc2_1$, $Cmcm$, and $C2cm$. Lattice parameters and systematic absences were consistent with those obtained previously by high-temperature X-ray powder diffraction.

Neutron diffraction has great advantages over X-ray diffraction in cases where the characterization of a low atomic number atom such as oxygen is of interest in a compound which also contains atoms of a much higher atomic number. Due to the unavailability of crystals of appropriate volume for single crystal neutron diffraction analysis, the Rietveld powder profile analysis technique was employed to solve the crystal structure. The sample powder was prepared by mixing the appropriate proportions of $La(OH)_3$ and Ta_2O_5 and firing at 1500°C, with intermediate grindings, until single phase material was obtained. This material was then annealed at 1750°C for 12 hr to improve crystallinity.

Neutron diffraction measurements were performed on a powder diffractometer at the NBS Reactor, with neutrons of wavelength 1.5416(3) Å. The horizontal divergence slits employed were 10 min of arc in the in-pile collimator, 20 min in the monochromatic beam collimator, and 10 min in the diffracted beam collimator. The sample powder was loaded into a vanadium can 1 cm in diameter which was in turn mounted in a vacuum furnace which was maintained at 300°C and 10^{-5} atm during the course of the data collection. Diffracted intensities were recorded between $2\theta = 5$ and 124°, at intervals of 0.05°. The diffractometer employed is equipped with five counters separated by 20° in 2-theta.

The powder profile refinement was performed via a local variation of the Rietveld program (*7*) adapted to the 5 detector diffractometer design and modified to allow the refinement of background intensity (*8*).

The neutron scattering amplitudes employed were $b(\mathrm{La}) = 0.83$, $b(\mathrm{Ta}) = 0.70$, and $b(\mathrm{O}) = 0.58$ ($\times 10^{-12}$ cm) (*9*). Initial lattice parameters were obtained by a least-squares fit to the observed positions of 10 low-angle peaks in the powder pattern, and initial values of the profile parameters U, V, and W were those obtained by Santoro *et al.* (*10*) in refinements of similar compounds. Approximate values of the background parameters were obtained at positions of the pattern free from diffraction effects. In the refinement of the final models, all structural, lattice and profile parameters were refined simultaneously. The refinement was considered terminated when all shifts were less than 0.3σ.

Results

Our initial model for the structure was centrosymmetric, based on the postulated

occurrence of nondistorted tantalum coordination octahedra. Atomic positions were determined from our knowledge of the low-temperature structure and our model for the phase transformation. Refinement in the space group *Cmcm* resulted in an agreement index, *Rw*, of 37%, which was considered unsatisfactory (see Table I for a definition of *Rw*). Relaxation of the tantalum coordination octahedra to a nonregular shape eliminated a set of mirror symmetries and placed the structure in the noncentrosymmetric space group $Cmc2_1$. Refinements in this space group converged to satisfactory agreement factors, with significant deviations of the tantalum coordination octahedra from regularity. The results indicated that $LaTaO_4$ at 300°C is isostructural with room temperature $BaMnF_4$, which has been the subject of extensive study due to its interesting physical properties (*11*) and the occurrence of a commensurate–incommensurate transition at low temperatures (*12*). In order that the results of this study might be easily compared with those of other compounds with the $BaMnF_4$ structure type, we report our results in the nonstandard space-group setting, $A2_1am$, which was chosen by Keve *et al.* (*13*) to follow the labeling convention $b > a > c$. All atoms were placed in the special positions 4*a*, point symmetry *m*, with coordinates of the type (*x*, *y*, 0). Structural, lattice, and profile parameters for the final structural model, in which isotropic thermal parameters were employed, are presented in Table I. The agreement index (*Rw*) for this model is 8.6%. The *x* parameters of the Ta and 04 atoms were strongly correlated. For the final model, 36 parameters were refined: 19 structural (including the scale factor), 4 lattice (including the 2θ zero point), 3 profile, and 10 background (slope and intercept parameters for linear profile background for each of the 5 detectors). Refinements employing anisotropic thermal vibration were also attempted and are described in a subsequent section.

TABLE I

FINAL STRUCTURAL, LATTICE, AND PROFILE PARAMETERS FOR $LaTaO_4$ AT 300°C

Ia. Space Group: $A2_1am$, $Z = 4$

Lattice parameters $a = 5.6643(1)$
$b = 14.6411(3)$
$c = 3.9457(1)$

Atom coordinates:

Atom	*x*	*y*	*z*	*B*
La	0.1788(6)	0.1676(2)	0.0	1.37(4)
Ta	0.2192(7)	0.4141(1)	0.0	0.68(4)
01	0.4216(7)	0.3008(2)	0.0	1.06(5)
02	−0.0486(7)	0.3380(2)	0.0	0.95(5)
03	0.5614(7)	0.4689(2)	0.0	1.42(7)
04	0.2496(7)	0.9153(3)	0.0	1.92(6)

R	*Rp*	*Rw*	*Re*	χ
7.74	6.53	8.56	4.49	1.91

where:

$$R = 100 \times \left\{ \frac{\Sigma |I(\text{obs}) - I(\text{calc})|}{\Sigma I(\text{obs})} \right\}$$

$$Rp = 100 \times \left\{ \frac{\Sigma |y(\text{obs}) - y(\text{calc})|}{\Sigma y(\text{obs})} \right\}$$

$$Rw = 100 \times \left\{ \frac{\Sigma w[y(\text{obs}) - y(\text{calc})]^2}{\Sigma w[y(\text{obs})]^2} \right\}^{1/2}$$

$$Re = 100 \times \left\{ \frac{N - P + C}{\Sigma w[y(\text{obs})]^2} \right\}^{1/2}$$

where N is the number of statistically independent observations, P is the number of parameters refined, C the number of constraints, y the number of counts at the angle 2θ, χ the ratio of weighted and expected R, I the integrated Bragg intensities, and w the weights.

Ib. Profile parameters $N - P = 3780$ $C = 0$

$U = .372(8)$
$V = -.43(1)$
$W = .193(3)$

The parameters U, V, and W appear in the equation:

$$H^2 = U \tan^2 \theta + V \tan \theta + W$$

where H is the full width at half maximum of a reflection occurring at the Bragg angle 2θ.

The final structure is shown in Fig. 1, a section in the (x, y, 0) plane. The cation–oxygen and oxygen–oxygen distances, as well as relevant bond angels, are presented in Table II. The tantalum ions are located near the center of the oxygen coordination octahedra, at an average bond distance of 1.98 Å. The distortion of the octahedra from regular shape is clearly indicated in

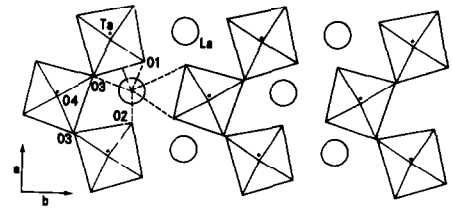

FIG. 1. The structure of $LaTaO_4$ at 300°C.

TABLE II

BOND DISTANCE AND ANGLES, $LaTaO_4$ AT 300°C

A. Distances

Tantalum octahedron		Oxygen–oxygen	
Ta–O1	2.02(1)	O3–O1	2.58(1)
O2	1.88(1)	O2	2.89(1)
O3	2.10(1)	O2	2.92(1)
O3	1.93(1)	O3	2.97(1)
O4	1.98(1)	O4	2.76(1)
O4	1.98(1)	O4	2.76(1)
Avg	1.98	O4	2.81(1)
		O4	2.81(1)
Lanthanum polyhedron		O4–O1	2.77(1)
		O2	2.83(1)
La–O1	2.39(1)	O2–O1	2.72(1)
O2	2.81(1)	O1	3.05(1)
O1	2.50(1)	O1	2.84(1)
O1	2.50(1)	Avg	2.79(1) within octahedron
O2	2.51(1)		
O2	2.51(1)		
O3	2.89(1)		
O3	2.89(1)		
O4	2.72(1)		
Avg	2.91		

B. Angles

Tantalum octahedron				Intra-octahedron			
O1	Ta	O3	77.8	Ta	O3	Ta	140.0
O1	Ta	O4	87.6	Ta	O4	Ta	170.0
O2	Ta	O1	88.4				
O2	Ta	O3	98.9				
O2	Ta	O4	94.3				
O3	Ta	O3	95.1				
O3	Ta	O4	85.2				
O3	Ta	O4	91.9				
O4	Ta	O4	170.0				

Fig. 1, and is reflected in the variation of the Ta–O bond distances and O–Ta–O bond angles presented in Table II.

The octahedra share corners only, and form sheets two octahedra wide that extend infinitely in the a and c directions. These sheets are aligned perpendicular to b, with alternate sheets displaced with respect to each other by 1/2 of an octahedron along c. Alternate sheets are held together by their bonding with the lanthanum ions, which are coordinated to seven oxygen ions in one sheet and two in the adjacent sheet. The average lanthanum–oxygen bond distance is 2.91 Å.

Finally, we note that in addition to the distortion of the tantalum–oxygen octahedra from regularity, octahedra which share corners to form the sheet spine parallel to a are canted with respect to each other. This is evidenced in the O1–O1–O1 bond angle which in an uncanted spine would be 180° and is, in this case, 144.4°, resulting in a more closely packed oxygen arrangement in the sheets.

Relation to the Low Temperature Structure and Model for the Phase Change

The low-temperature form of $LaTaO_4$ is monoclinic, centrosymmetric space group $P2_1/c$, with the unit cell parameters a = 7.651 Å, b = 5.577 Å, c = 7.823 Å, and β = 101°31′ (*3*). A projection of the structure parallel to its c axis is presented in Fig. 2, a projection that allows easy comparison to the orthorhombic form.

The tantalum–oxygen octahedra do not change shape or dimension substantially on cooling from the orthorhombic to the monoclinic form. The only significant change is a small increase in the height of the octahedra parallel to the orthorhombic c direction, and a corresponding deequalization of the Ta–O4 bond distances. The coordination of the lanthanum ions does

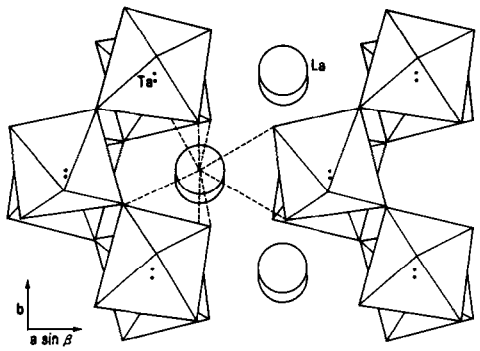

FIG. 2. The structure of $LaTaO_4$ at 25°C (*3*).

change, however, and is intimately related to the reorientation of the tantalum coordination octahedra with respect to each other.

The three major reorientations which occur all involve rotation of the octahedra through axes passing through their shared corners: (1) the O4–O4 axes of the octahedra, which are parallel to c and each other in the orthorhombic form, become skew with respect to c and each other in the monoclinic form. This effectively relaxes the coplanar oxygen arrays at z = 0 and 1/2 in the orthorhombic form to noncoplanar arrays. (2) a rotation of alternate octahedra along c about an axis parallel to c and passing through the shared corners (O4 atoms) such that they are no longer aligned but are rotated 22° with respect to each other. This effectively doubles the c axis. (3) Finally, the angle of the octahedra-spine increases from about 144.4° in the orthorhombic form to 149° in the monoclinic form.

These geometrical changes in the sheets of tantalum–oxygen octahedra result in major changes in the coordination of the lanthanum ion. In the high temperature phase the coordination is ninefold. In cooling through the orthorhombic to monoclinic transformation, two of the coordinating oxygen ions in the spine of the sheets of octahedra move significantly further away

and one moves closer, resulting in a decrease in coordination from 9 to 8. This coordination is illustrated in Fig. 2. A comparison of the lanthanum–oxygen bond distances indicates a general decrease in the average (2.64 to 2.54) on transformation. The bonding lengths to the two oxygen ions in the adjacent sheet do not change significantly. The large variation in orthorhombic to monoclinic transition temperatures for the lanthanum, cerium, and praseodymium tantalates is no doubt related to the ease with which these changes in geometry occur. The variation is difficult to rationalize in terms of the rare earth ionic radii, which change by only 3% between La and Pr, though more complex changes have been noted for other rare earth oxides over similar ranges in radius (*14*).

The geometrical changes described above result in a lowering of symmetry from $A2_1am$ to $P2_1/c$ with the gain of a center of symmetry. The monoclinic and orthorhombic cells are related by

$$a_{\text{mon}} = 1/2\ (b_{\text{orth}} + c_{\text{orth}})$$
$$b_{\text{mon}} = a_{\text{orth}}$$
$$c_{\text{mon}} = -2c_{\text{orth}}$$

with small contractions (on cooling) in dimension along the orthorhombic a and c axes, and a small expansion along b, the dimension perpendicular to the sheets. The unit cell volume does not change significantly. The dimensional changes result in a small decrease in the angle between the [001] and [011] directions in the orthorhombic and the corresponding [001] and [100] directions in the monoclinic from 105.1 to 101.5°, the β angle. An earlier study (*4*) of the variation of unit cell parameters with temperature at 10°C intervals near the phase transition leads us to tentatively identify the orthorhombic to monoclinic transition as being first order.

Relation to $BaMnF_4$ and Other Compounds

Several compounds display structures which are similar to that of $LaTaO_4$. Both triclinic β-$BiNbO_4$ (*19*) and monoclinic $NaNbO_2F_2$ (*20*) are similar to monoclinic $LaTaO_4$. Our studies indicate that these compounds might well display transitions to higher symmetry structures, possibly with the orthorhombic $LaTaO_4$ structure, at elevated temperatures.

As $BaMF_4$ compounds (where M = Mn, Fe, Co, Ni, and Zn) have been studied extensively, comparison to $LaTaO_4$, especially of $BaMnF_4$ where the most careful structural work has been done, is of great interest. The similarity of the structures can be seen in terms of the coordinates presented in Table III. The x coordinates of the atoms in $BaMnF_4$ have been taken from the work of Keeve *et al.* and translated along a such that X_{Mn} and X_{Ba} are equal (the origin of the structure is not uniquely defined). The differences are surprisingly small, the largest being in the y coordinates of the Ba and La atoms. This is related to the manner in which the Ba and La bond neighboring sheets of octahedra to each other. Keeve *et al.* in fact concluded that barium is coordinated to 1 fluorine in the adjacent sheet, whereas we must conclude that lanthanum is coordinated to 2 oxygen

TABLE III

FRACTIONAL ATOMIC COORDINATES IN $BaMnF_4$ AND $LaTaO_4$ REFERRED TO THE $LaTaO_4$ COORDINATE SYSTEM AND LATTICE PARAMETERS

Atoms	$BaMnF_4$	$LaTaO_4$
Ba, La	(0.173, 0.157, 0)	(0.179, 0.168, 0)
Mn, Ta	(0.219, 0.146, 0)	(0.219, 0.414, 0)
F1, O1	(0.415, 0.298, 0)	(0.422, 0.301, 0)
F2, O2	(−0.156, 0.336, 0)	(−0.049, 0.338, 0)
F3, O3	(0.556, 0.465, 0)	(0.561, 0.469, 0)
F4, O4	(0.235, 0.922, 0)	(0.250, 0.915, 0)
a (A)	5.9845(3)	5.6643(1)
b (A)	15.098(2)	14.6411(3)
c (A)	4.2216(3)	3.9457(1)

in that sheet. The difference in the x coordinates of the F4 and O4 ions is related to the difference in shape of the Ta and Mn coordination octahedra.

The results of Keeve *et al.* for room temperature $BaMnF_4$ reveal very high anisotropies in the thermal motion of some of the atoms. Table IV presents the atomic principal mean square displacements which we calculated from their published lattice parameters and β matrix transformed to its principal axes. Many of the thermal parameters are unusually large for a structure at room temperature. Anisotropies in mean square displacements of a factor of 4 are large, but not anomalous. The anisotropy ratios of 9.32 and 71.6 for the F4 and F3 ions, respectively, however, especially in connection with one very small principal mean square displacement for F3, are indicative of peculiarities and perhaps disorder in the structure.

We tested for the presence of anisotropic thermal vibrations in $LaTaO_4$ with the powder profile refinement. With all atoms allowed to be anisotropic, 18 structural parameters were added to the refinement and *Rw* dropped from 8.56 to 7.2. Three of the six atoms were then determined not to be significantly anisotropic. In the refinement in which only the La, Ta, and O4 atoms were taken as anisotropic the *Rw* dropped to 7.3%. The thermal parameters for this model are presented in Tables V, along with the principal mean square displacements and anisotropy ratios. The anisotropies for La and Ta are larger but comparable to those reported for Ba and Mn in $BaMnF_4$. On the other hand, only the O4 ion displays an anomalously high anisotropy coupled with one very small principal mean square displacement.

TABLE IV

PRINCIPAL MEAN SQUARE DISPLACEMENTS IN $BaMnF_4$ AT ROOM TEMPERATURE

Atom	MSD(1)Å²	MSD(2)Å²	MSD(3)Å²	Maximum anisotropy
Ba	0.0376	0.0132	0.0093	4.04
Mn	0.0179	0.0106	0.0089	2.01
F1	0.0316	0.0298	0.0073	4.33
F2	0.0315	0.0217	0.0198	1.59
F3	0.0599	0.0451	0.00084	71.6
F4	0.0758	0.0354	0.0081	9.32

It was initially believed that these thermal parameters might be indicative of the presence of static disorder. A stacking fault, for instance, in which some fraction of the crystal retained the alternating skew octahedra parallel to c characteristic of the monoclinic form to high temperatures might show as anomalous thermal parameters in the structural refinement. To test this hypothesis, the atom positions for a stacking fault actually suggested in the discussion of the $BaMnF_4$ structure by Keeve *et al.* were generated from the final positional parameters obtained for $LaTaO_4$ by reflection of the positions across mirror planes perpendicular to a and passing through the Ta atoms. The refinement of the percentage of such stacking faults was stable and their number was found not to be significantly different from zero. We feel justified, therefore, in rejecting the possibility of stacking faults of this type in $LaTaO_4$ at 300°C.

The highly anisotropic vibrations might be explained in terms of possible phonon modes of the structure. Oscillations of the corner linked Mn or Ta coordination octahedra about axes parallel to c and through their centers would account for the severely flattened thermal elipsoids observed for the F3 atoms in $BaMnF_4$, and oscillations of the octahedra about axes perpendicular to c for the severely flattened elipsoids of the F4 and O4 atoms in both $BaMnF_4$ and $LaTaO_4$. Similar anisotropies have been observed for the anions in the corner-linked octahedra in $CsPbCl_3$ (*15*), which has the perovskite structure. In that case, the oscillations of the $PbCl_6$ octahedra have been related to soft phonon modes

TABLE Va

THERMAL PARAMETERS: $LaTaO_4$ AT 300°C, THREE ANISOTROPIC ATOMS

Atom	B11	B22	B33	B23	B or equiv. B	B isotropic model
La	0.37(6)	2.24(8)	1.64(8)	−0.33(8)	1.42	1.37(4)
Ta	0.30(7)	1.06(10)	0.45(9)	−0.08	0.60	0.68(4)
O1					1.02(4)	1.06(5)
O2					1.08(4)	0.95(5)
O3					1.67(5)	1.42(7)
O4	0.14(8)	2.70(12)	3.01(14)	0.48(11)	1.95	1.92(6)

which drive a structural phase transition. $BaMnF_4$ has also been shown to exhibit soft mode behavior near its structural phase transition (*12*). These considerations lead us to interpret the disorder implied by the thermal parameters in $LaTaO_4$ at 300°C and $BaMnF_4$ at room temperature as being related to the actual thermal motion of the atoms. We believe that the atomic motions are likely to be severely anharmonic in both compounds. Due to the limitations of the powder data, we were unable to test this hypothesis for $LaTaO_4$.

Doubling of the magnetic unit cell has been observed in orthorhombic $BaCoF_4$, $BaMnF_4$, $BaNiF_4$, and $BaFeF_4$ at low temperatures, in both the *b* and *c* directions (12, 16, 17, 18). This has been attributed to oppositely directed magnetic moments along *a* in $BaCoF_4$, *b* in $BaNiF_4$ and $BaFeF_4$, and 9° from *b* in $BaMnF_4$. The additional magnetic reflections at $(h, k + 0.5, l + 0.5)$ require the assignment of the monoclinic space group $P2_1$. This reciprocal lattice is identical to that in monoclinic $LaTaO_4$ except for a small angular distortion and the presence of reflections with *l* odd on one zero level ($(0kl)$ in the orthorhombic-based cell) due to the absence of a glide plane. The neutron diffraction data on the $BaMF_4$ compounds at low temperatures apparently do not suggest that the *b* and *c* axis doublings are related to the relaxation of the orientations of the MX_6 octahedra as they are in $LaTaO_4$.

$BaMnF_4$ undergoes a commensurate to incommensurate phase transition at 247°K. Neutron diffraction studies (*12*) have shown that the incommensurate phase is characterized by additional reflections at points in reciprocal space which are multiples of (0.39, 0.5, 0.5). We have very carefully inspected the powder pattern for $LaTaO_4$ at 300°C and have observed no incommensurate reflections. A physical picture of the incommensurability along *a* in $BaMnF_4$ has not yet been proposed. It is indeed difficult to do so based on the relationship between high and low temperature $LaTaO_4$, except that is might be related to either the straightening or kinking of the angle in the spine of the sheets of octahedra parallel to *a*, or relaxations or rotations of the octahedra of the type that have been described here.

TABLE Vb

PRINCIPAL MEAN SQUARE DISPLACEMENT IN $LaTaO_4$ AT 300°C, ANISOTROPIC ATOMS

Atom	MSD(1) Å²	MSD(2) Å²	MSD(3) Å²	Maximum anistropy
La	0.0302	0.0189	0.0047	6.37
Ta	0.0136	0.0056	0.0038	3.57
04	0.0426	0.0298	0.0017	24.4

Conclusions

Our neutron diffraction powder profile analysis of $LaTaO_4$ at 300°C has shown it to be isostructural with room temperature $BaMnF_4$. Based on the great similarity in lattice parameters and X-ray powder diffraction patterns we can conclude that the orthorhombic phases of $CeTaO_4$ and $PrTaO_4$ have the same structure. Several of the atoms display strongly anisotropic and probably anharmonic thermal motions. Despite the great similarities between the structures of the orthorhombic $LaTaO_4$ and $BaMF_4$ type compounds, they apparently undergo transitions to different structures at low temperatures.

Acknowledgment

The authors wish to thank Dr. A. Santoro for help and advise on the use of the neutron diffraction equipment and the structure refinement by the total profile analysis technique.

References

1. K. A. Gingerich and H. E. Blair, *Adv. X-ray Anal.* **7**, 22 (1963).
2. R. S. Roth, T. Negas, H. S. Parker, D. B. Minor, and C. Jones, *Mat. Res. Bull.* **12**, 1173 (1977).
3. T. A. Kurova and V. B. Akesandrov, *Dokl. Akad. Nauk. SSSR* **201**, [5] 1095 (1971).
4. R. J. Cava, R. S. Roth, T. Negas, and D. B. Minor, *in* "The Rare Earths in Modern Science and Technology" (G. J. McCarthy and J. J. Rhyne, Eds.), p. 181. Plenum Press, New York (1978).
5. T. Negas, R. S. Roth, C. L. McDaniel, H. S. Parker, and C. D. Olson, *Mat. Res. Bull.* **12**, 1161 (1977).
6. R. J. Cava and R. S. Roth, *IN* "Proceedings of the Conference on Modulated Structures, Honolulu, Hawaii" (1979).
7. H. M. Rietveld, *J. Appl. Crystalogr.* **2**, 65 (1969).
8. E. Prince, to be published.
9. "International Tables for X-ray Crystallography," Vol. IV. Kynoch Press, Birmingham (1974).
10. A. J. Santoro, M. Marezio, and R. S. Roth, *J. Solid State Chem.* (1981) in press.
11. See for instance, M. Eibschutz, H. Guggenheim, S. Wemple, I. Camlibel, and M. DiDomenico, *Phys. Lett.* **29**, 409 (1969).
12. D. E. Cox, S. Shapiro, R. Cowley, M. Eibschutz, and H. Guggenheim, *Phys. Rev.* **B19**, 5754 (1979).
13. E. T. Keve, S. C. Abrahams, and J. L. Bernstein, *J. Chem. Phys.* **51**, 4928 (1969).
14. R. S. Roth, and S. J. Schneider, *J. Res. NBS* **64A**, 317 (1960).
15. J. Marada, M. Sakata, S. Hoshino, and S. Hirotsu, *J. Phys. Soc. Japan* **40**, 212 (1976).
16. M. Eibschutz, L. Holmes, H. Guggenheim, and D. Cox, *J. Phys.* **32**, C1-759 (1971).
17. M. Eibschutz, L. Holmes, H. Guggenheim, and D. Cox, *Phys. Rev.* **B6**, 2677 (1972).
18. D. E. Cox, M. Eibschutz, H. Guggenheim, and L. Holmes, *J. Appl. Phys.* **41**, 943 (1970).
19. E. T. Keve and A. C. Skapski, *J. Solid State Chem.* **8**, 159 (1973).
20. S. Andersson and J. Galy, *Acta Crystallogr.* **B25**, 847 (1969).